ELSEVIER

International Journal of Solids and Structures 41 (2004) 2165–2188

INTERNATIONAL JOURNAL OF SOLIDS and STRUCTURES

www.elsevier.com/locate/ijsolstr

Interpolations for temperature distributions: a method for all non-concave polygons

Elisabeth Anna Malsch *, Gautam Dasgupta

Department of Civil Engineering and Engineering Mechanics, Columbia University, 500 West 120th St., New York, NY 10027, USA

Received 25 June 2002; received in revised form 20 August 2003

Abstract

An approximation to a distribution governed by temperature readings taken at the edge of a polygonal domain can be constructed using interpolation functions which—in linear combination—satisfy first order, constancy and linearity conditions. The values prescribed by the normed interpolation function should be bounded between zero and one. This restriction is especially necessary when representing temperature, since negative values for temperature in Kelvin are physically unacceptable. Compliant interpolation functions can be constructed on all convex polygonal domains including those bounded by vertex and side-nodes.

Keywords: Temperature distribution; Side-node; Shape function; Isoparametric; Degenerate element

1. Introduction

Continuous problems governed by limited data require interpolation functions which capture as many of the known properties of the distributed quantity as possible. In the case of heat flow the smoothness and boundedness of the solution is well documented. Consequently, the assumed function should be greater or equal to the smallest nodal value and less than or equal to the greatest nodal value throughout the domain. Physical impossibilities, such as negative Kelvin, are avoided by such a representation. Also, temperature distributions are necessarily minimum or maximum only along the boundary. Any discretization which mars this smoothness should be avoided.

Additionally, an assumed interpolation should represent the one dimensional behavior of the boundary. In a steady state temperature problem the one dimensional distribution of temperature between heat sources is linear, the behavior along the boundary of a two dimensional domain should similarly be linear (Haberman, 1998, pp. 13–15). Conventional interpolations and test functions do not consistently satisfy these requirements (see Table 1).

* Corresponding author.
E-mail address: malsch@civil.columbia.edu (E.A. Malsch).

0020-7683/$ - see front matter © 2003 Elsevier Ltd. All rights reserved.
doi:10.1016/j.ijsolstr.2003.11.037

Table 1
Comparison of conventional approaches

Method	Weakness	Strength
Displacement based finite element method: Triangular or quadrilateral mesh	• Requires mesh • Not smooth • 3 or 4 nodes only	• Bounded
Large element methods: Lagrange or Coon's element	• Unbounded • Only specific shapes	• No mesh • Smooth
Boundary element method	• Needs field equation solution • Results along the boundary are approximate	• No mesh

The goal then is to construct a large element interpolation which is necessarily bounded, linear along the edges and applies generally to different shapes. Any non-concave polygon with any number of nodes and side-nodes can be represented by a bounded smooth function. The limitations of conventional displacement finite element formulations are due in part to the arbitrary requirement that such functions be polynomial in form (Courant, 1943). By extending the domain of functions to include rational and even irrational polynomials algebraic shape functions for any polygonal area can be constructed.

2. Interpolation requirements

Given a set of shape functions $\phi_i(x,y)$ associated with the vertex coordinate $\{x_i, y_i\}$; define the shape function such that each is single valued at its named coordinate:

$$\phi_i(x_j, y_j) = \delta_{ij} = \begin{cases} 1 & i = j, \\ 0 & i \neq j. \end{cases} \tag{1}$$

Along the boundary adjacent to the single valued node the behavior should be linear. Let the adjacent node, traveling cyclically around the boundary, be node $\{x_k, y_k\}$:

$$\phi_k(x_k t + x_j(1-t), y_k t + y_j(1-t)) = t. \tag{2}$$

Within the domain defined by the vertices $\mathscr{D}$, the shape function should be smooth, bounded and be able, in linear combination, to reproduce constant and linear fields, then $\forall\{x,y\} \in \mathscr{D}$ (Irons and Ahmad, 1980):

$$0 < \phi_i(x,y) < 1, \tag{3}$$

$$\sum_{i=1}^{n} \phi_i(x,y) = 1, \quad \sum_{i=1}^{n} x_i \phi_i(x,y) = x \quad \text{and} \quad \sum_{i=1}^{n} y_i \phi_i(x,y) = y. \tag{4}$$

Any smooth function which satisfies these requirements can be used to approximate a temperature distribution.

2.1. Polynomial shape functions

Rectangular and triangular $\mathbb{C}^0$ shape functions do satisfy these interpolation requirements within elements governed by three or four nodes respectively. The shape functions are polynomials in normed coordinates $\{\xi, \eta\}$.

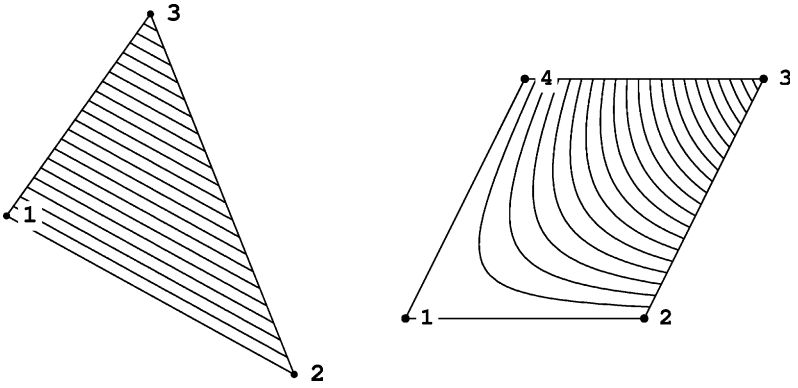

Fig. 1. Shapes with polynomial interpolations.

$$\begin{aligned}&\text{Triangle}: \quad \phi^t(\xi,\eta) = a_3\eta + a_2\xi + a_1\\ &\text{Rectangle}: \quad \phi^r(\xi,\eta) = b_4\eta\xi + b_3\eta + b_2\xi + b_1\end{aligned} \tag{5}$$

The constant coefficients $\{a_1, a_2, a_3\}$ and $\{b_1, b_2, b_3, b_4\}$ are defined by the geometry of the domain and the general shape function requirements according to Courant's triangle (1943) and Taig's quadrilateral (1961) (see Fig. 1).

$$\phi_a^t(\xi,\eta) = \frac{\triangle(\vec{\xi}, b, c)}{\triangle(a,b,c)}, \quad \forall\{\xi,\eta\} \in \triangle(a,b,c) \tag{6}$$

and

$$\phi_i^r(\xi,\eta) = \frac{(1 \pm \xi)(1 \pm \eta)}{4}, \quad \forall\{\xi,\eta\} \in (-1,1). \tag{7}$$

Using the area coordinate representation the positivity of the interpolation can be discerned by inspection. The area of a triangle whose vertices lie at the points $\{a,b,c\}$ is labeled $\triangle(a,b,c)$. Similarly $\triangle(\vec{x},b,c)$ is the area of the triangle whose vertices lie at points $\{x,y\}$, $\{x_b,y_b\}$ and $\{x_c,y_c\}$ respectively.

$$\triangle(a,b,c) \stackrel{\wedge}{=} \frac{1}{2}\begin{vmatrix} x_a & y_a & 1\\ x_b & y_b & 1\\ x_c & y_c & 1\end{vmatrix} \quad \text{and} \quad \triangle(\vec{x},b,c) \stackrel{\wedge}{=} \frac{1}{2}\begin{vmatrix} x & y & 1\\ x_b & y_b & 1\\ x_c & y_c & 1\end{vmatrix}. \tag{8}$$

Also, the function $\triangle(\vec{x},b,c)$ is zero valued along the line passing through the points b and c. The determinant form is signed. If the vertices are arranged in a positive sense then the area is positive, otherwise it is negative (Irons and Ahmad, 1980).

2.2. Rational polynomial formulation

The rational polynomial form is more flexible. It can be used to represent first order interpolations within any convex two dimensional shapes. The shape function formulation for any convex polygon can be derived generally as an algebraic collection of functions which are appropriately zero valued and linear around the boundary lines (see Fig. 2) (Dasgupta, 2003b). Define a function $s_i(x,y)$ such that the function is zero along all boundary lines except those adjacent to node i.

$$s_{i\neq j \,\&\, i\neq j-1}(x_j + t(x_{j+1} - x_j), y_j + t(y_{j+1} - y_j)) = 0, \quad \forall t \in (0,1). \tag{9}$$

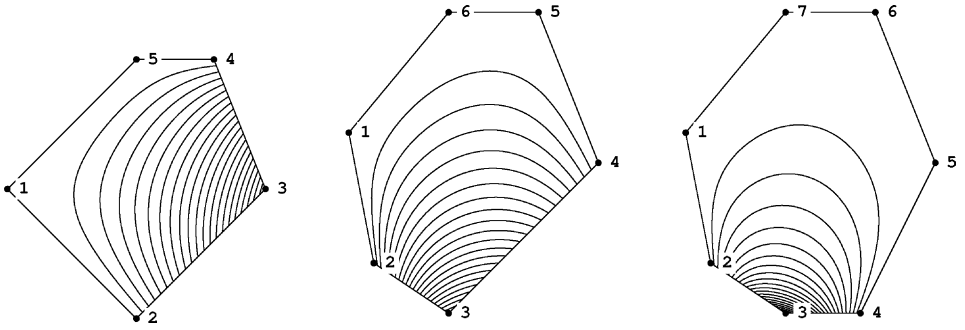

Fig. 2. Shapes with rational polynomial interpolations.

The product of functions which are zero on each of the non-adjacent boundary lines satisfies this criteria.

$$l_i(x,y) = Ax + By + C \quad \text{and} \quad l_i(x_i,y_i) = l_i(x_{i+1},y_{i+1}) = 0. \tag{10}$$

solving for A and B, C is an arbitrary scaling factor, find,

$$l_i(x,y) = D\triangle(\vec{x}, i, i+1). \tag{11}$$

Let the arbitrary constant $D = 1$. Define:

$$r(x,y) = \prod_{j=1}^{n} l_j(x,y) \quad \text{then } s_i(x,y) = \frac{r(x,y)}{l_i(x,y)l_{i-1}(x,y)}, \tag{12}$$

where, n is the number of nodes and the numbering is cyclic, e.g. point $i = 0$ and point $i = n$ are the same point. The resulting shape function is

$$N_i(x,y) = \frac{k_i s_i(x,y)}{\sum_{j=1}^{n} k_j s_j(x,y)}. \tag{13}$$

The sum of all shape functions is one, this satisfies the constancy requirement (see Eq. (4)). Along the edges adjacent to node-i the function should be linear along the boundary.

$$N_i(x_i + t(x_{i+1} - x_i), y_i + t(y_{i+1} - y_i)) = Dt + E. \tag{14}$$

The relationship between k_i and k_{i+1} can be derived from this condition.

$$k_{i+1}\triangle(i-1, i, i+1) = k_i\triangle(i, i+1, i+2). \tag{15}$$

Consequently, the linear edge requirement is satisfied if the constants are defined in terms of the vertex areas:

$$k_j = \triangle(j-1, j, j+1). \tag{16}$$

Since $\triangle(a,b,c)$ is the area of the triangle whose nodes are in cyclic order, the constants are necessarily positive. The method applies to any convex element with any number of nodes. It does not apply to concave elements since the elongations of the boundary lines would prescribe zero values inside the domain.

The bounded linear edged interpolation within any convex element with any number of nodes is:

$$N_j^n(x,y) = \frac{\triangle(j-1,j,j+1)\left(\prod_{\forall k\neq j \text{ or } j-1} \triangle(\vec{x},k,k+1)\right)}{\sum_{i=1}^{n}\triangle(i-1,i,i+1)\left(\prod_{\forall k\neq i \text{ or } i-1} \triangle(\vec{x},k,k+1)\right)}. \tag{17}$$

Alternatively, this shape function representation can derived from projective geometry using external intersection points (Wachspress, 1975). The solutions are valid within any convex quadrilateral domain. The same rational polynomial form results.

The shape function for a triangle is also derivable from this formula. The general shape function for node a of a convex quadrilateral (a,b,c,d) is:

$$N_a^4(x,y) = \frac{\triangle(d,a,b)\triangle(\vec{x},b,c)\triangle(\vec{x},c,d)}{\left(\begin{array}{c}\triangle(d,a,b)\triangle(\vec{x},b,c)\triangle(\vec{x},c,d)+\triangle(a,b,c)\triangle(\vec{x},c,d)\triangle(\vec{x},d,a)\\ +\triangle(b,c,d)\triangle(\vec{x},d,a)\triangle(\vec{x},a,b)+\triangle(c,d,a)\triangle(\vec{x},a,b)\triangle(\vec{x},b,c)\end{array}\right)}. \tag{18}$$

The interpolation constructed for any trapezoid is equal to that found by isoparametric transformation. The emergence of rational and even irrational polynomial forms is evident from the isoparametric transformation. The projective geometry foundation for such formulations is discussed by Wachspress (1975).

2.3. Irrational polynomial formulation

On a one dimensional domain a piecewise linear interpolation describes the temperature distribution in a bar subject to point sources exactly. Similarly, a boundary subject to the same point loading should exhibit the same behavior. The simplest algebraic formulation which represents a gradient discontinuity is:

$$\sqrt{x^2} = |x|.$$

Multiple discontinuities can be modeled as well:

$$\sqrt{(1-\sqrt{x^2})^2} = |1-|x||.$$

The functions are plotted in Fig. 3. The irrational, polynomial characterized by the square root can model piecewise linear behavior. The polynomial and rational polynomial alone are insufficient.

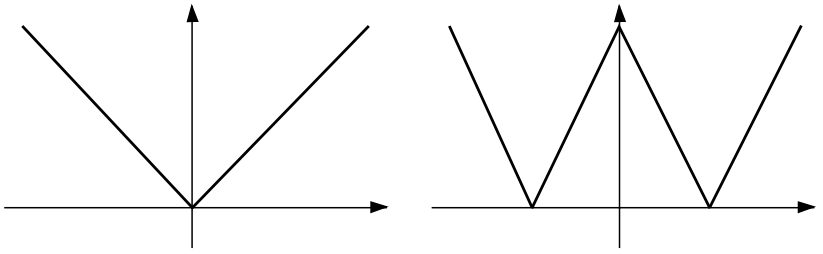

Fig. 3. Gradient discontinuity.

3. Isoparametric transformation in x–y coordinates

The limits and extents of the isoparametric formulation for a four-noded finite element are derived by transforming the parametrized shape function from ξ–η to x–y coordinates. This analytic inversion results in a quadratic equation. The coefficients of this equation dictate whether the form of the shape function is a polynomial, a rational polynomial or an expression containing a square root.

The shape function for a triangular element need not be constructed in a computational frame $\{\xi, \eta\}$ it can be constructed in local $\{x, y\}$ coordinates directly:

$$\phi_a^t(x,y) = \frac{\triangle(\vec{x}, b, c)}{\triangle(a, b, c)}, \quad \forall\{x,y\} \in \triangle(a,b,c).$$

In the Taig quadrilateral formulation the local coordinates are a function of the $\{\eta, \zeta\}$;

$$x = \sum_{i=1}^{n} x_i N_i(\xi,\eta) \quad \text{and} \quad y = \sum_{i=1}^{n} y_i N_i(\xi,\eta). \tag{19}$$

Consequently, any shape functions resulting from the transformation satisfy the linearity requirements (see Eq. (4)).

Let $\{s, t\}$ parametrize the Cartesian $\{x, y\}$ coordinates according to:

$$\begin{aligned} &N_1(s,t) = (1-s)(1-t), \quad N_2(s,t) = s(1-t), \\ &N_3(s,t) = st, \quad N_4(s,t) = (1-s)t. \end{aligned} \tag{20}$$

The formulation is the same as Eq. (7), except that the unit square is shifted such that $s \in (0,1)$ and $t \in (0,1)$. Let the equation for the third node be $\phi_c = N_3(s(x,y), t(x,y))$. Solving for the shape function ϕ_c in terms of x and y using Eq. (19), the resulting equation is a quadratic in ϕ_c (see Appendix A.1 for a specific example):

$$\alpha\phi_c^2 - \beta(x,y)\phi_c + \gamma(x,y) = 0, \tag{21}$$

where the coefficients are polynomials in (x, y):

$$\begin{aligned} \alpha &= (\triangle(d,a,b) - \triangle(a,b,c))(\triangle(d,a,b) - \triangle(c,d,a)), \\ \beta(x,y) &= \triangle(d,a,b)^2 - \triangle(\vec{x},d,a)(\triangle(d,a,b) - \triangle(a,b,c)) - \triangle(\vec{x},a,b)(\triangle(d,a,b) - \triangle(c,d,a)), \\ \gamma(x,y) &= \triangle(\vec{x},d,a)\triangle(\vec{x},a,b). \end{aligned} \tag{22}$$

The coefficient α is constant, $\beta(x,y)$ is linear and $\gamma(x,y)$ is quadratic in x and y. The area coordinate representation (Eq. (21)) shows that the quantities must be positive within any non-concave shape. If the shape is non-concave the areas described by $\triangle(i,j,k)$ are zero or positive if the node numbering is in a positive sense.

3.1. Quadrilateral test case

The quadrilateral element can exhibit skewness, concavity and a side-node. The isoparametric transformation applies only to non-concave shapes.

In a parallelogram (a, b, c, d) the subtriangles created by connecting opposite vertices are equal in area (see Fig. 4):

$$\triangle(d,a,b) = \triangle(a,b,c) \quad \text{and} \quad \triangle(d,a,b) = \triangle(c,d,a).$$

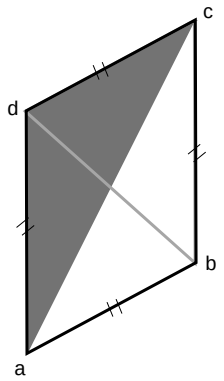

Fig. 4. Parallelogram.

For the parallelogram, the constant α is zero and The equation for $\beta(x,y)$ is constant:

$$\beta(x,y) = \triangle(d,a,b)^2.$$

For this case, the shape functions derived using projective geometry and parametric coordinates are the same. The shape function is indeed a polynomial:

$$\phi_a(x,y) = \frac{\triangle(\vec{x},d,a)\triangle(\vec{x},a,b)}{\triangle(d,a,b)^2}; \tag{23}$$

also,

$$s = \frac{\triangle(\vec{x},d,a)}{\triangle(d,a,b)} \quad \text{and} \quad t = \frac{\triangle(\vec{x},a,b)}{\triangle(d,a,b)}. \tag{24}$$

In a trapezoid (a,b,c,d), see Fig. 5, the subtriangles created by connecting opposite vertices are equal in area:

$$\triangle(d,a,b) = \triangle(c,d,a).$$

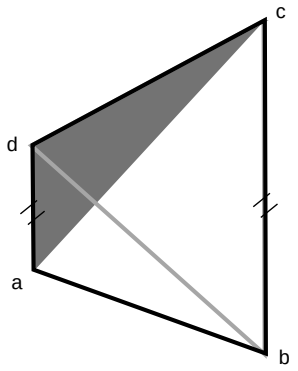

Fig. 5. Trapezoid.

Again, the constant α is zero. Similarly:

$$\beta(x,y) = \triangle(d,a,b)^2 - \triangle(\vec{x},d,a)(\triangle(d,a,b) - \triangle(a,b,c)).$$

For the trapezoidal case, the shape function found using projective geometry and parametrized coordinates are equal. The shape function is in rational polynomial form:

$$\phi_a(x,y) = \frac{\triangle(\vec{x},d,a)\triangle(\vec{x},a,b)}{\triangle(d,a,b)^2 - \triangle(\vec{x},d,a)(\triangle(d,a,b) - \triangle(a,b,c))}. \tag{25}$$

For a quadrilateral with no parallel sides α is not zero. For a convex quadrilateral the solution can be constructed as a rational polynomial using the Wachspress method. Or, a result can be found using parametrized coordinates as the branching solution of the roots of a quadratic equation:

$$\phi_a(x,y) = \frac{\beta(x,y) \pm \sqrt{\beta(x,y)^2 - 4\alpha\gamma(x,y)}}{2\alpha}. \tag{26}$$

On a convex skew quadrilateral the boundary conditions are not satisfied by booth roots. On the boundary $\overline{\mathbf{da}}$ and $\overline{\mathbf{ba}}$ the linear terms vanish and $\beta(x,y) > 0$. The negative root is zero, $(\beta(x,y) - \sqrt{\beta(x,y)^2} = 0)$ and the positive root is a positive constant $(\beta(x,y) + \sqrt{\beta(x,y)^2} = 2\triangle(d,a,b)^2)$. Along the boundary $\overline{\mathbf{bc}}$ (Fig. 6):

$$\begin{aligned} &\triangle(\vec{x},d,a) \to (1-t)\triangle(b,d,a) + t\triangle(c,d,a), \\ &\triangle(\vec{x},a,b) \to (1-t)\triangle(b,a,b) + t\triangle(c,a,b). \end{aligned} \tag{27}$$

The discriminant term becomes:

$$\triangle(d,a,b)^2\triangle(c,a,b) + t(\triangle(c,d,a) - \triangle(d,a,b))^2. \tag{28}$$

The value of the negative root then is linear in t, $\phi_c(x_b(1-t) + x_c(t)) = t$. The result is similar for the boundary $\overline{\mathbf{cd}}$. The negative root at point c then is unit valued: $\phi_c(x_c, y_c) = 1$. The negative root satisfies the boundary conditions:

$$\phi_c(x,y) = \frac{\beta(x,y) - \sqrt{\beta(x,y)^2 - 4\alpha\gamma(x,y)}}{2\alpha}. \tag{29}$$

For a specific example see Appendix A.2.

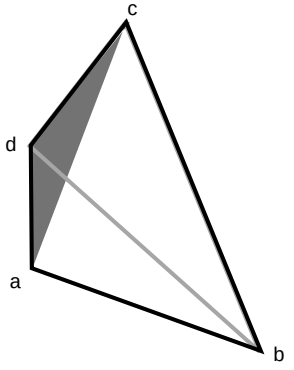

Fig. 6. Skew.

4. Form of the shape function

In 1975, Wachspress introduced a rational polynomial formulation for finite elements which applies consistently to any convex n-sided polygon; it does not apply to elements with a side-node. The same publication describes irrational shape functions (Wachspress, 1975, pp. 245–253). Similar to the isoparametric transformation, a shape function is calculated by projecting a three dimensional shape on a two dimensional plane. Unlike the presented method, Wachspress' three dimensional shape is curved. The shape function for the side-node is calculated, and promptly canceled out of the representation. The linear boundary conditions are not captured along the edge with the side-node. Nevertheless, some ingenious, non-convex, elements with curved sides can be constructed.

Wachspress realized the limitations of the rational polynomial formulation with respect to "ill-set elements", non-convex polygons and polycons (Wachspress, 1975, p. 247). Just as the polynomial shape function cannot be applied to more than a few basic shapes, the rational polynomial method also fails when a polygon is non-convex.

Following the series of Hermite–Padé type approximations leads to a quadratic form, and an irrational shape function. Any piecewise continuous function can be represented by an infinite power series

$$f(x) = \sum_{n=0}^{\infty} a_n x^n, \quad a_0 \neq 0, \quad |x| < R. \tag{30}$$

The Padé approximate of the same function can be written as:

$$\sum_{n=0}^{k} \beta_n x^n f(x) - \sum_{n=0}^{j} \gamma_n x^n = \mathrm{O}(x^{(j+k+1)}), \tag{31}$$

where $\mathrm{O}(\cdot)$ is an order operator. The coefficients β_i and γ_i are functions of the coefficients of the power series a_i. The approximation is valid if the function is not evaluated near the denominator zeros ($\sum_{n=0}^{k} \beta_n x^n = 0$) (Shafer, 1974). The zeros of the denominator lie strictly outside the convex polygonal domain in the rational polynomial representation (Wachspress, 1975).

A polynomial representation cannot satisfy the boundary conditions of a polygon which is not sufficiently symmetric. The rational polynomial form cannot be used to satisfy the boundary conditions in a non-convex polygon. The next order construction is known as the *Quadratic Shafer* or *Hermite–Padé* approximate:

$$\sum_{n=0}^{l} \alpha_n x^n f(x) - \sum_{n=0}^{k} \beta_n x^n f(x) + \sum_{n=0}^{j} \gamma_n x^n = \mathrm{O}(x^{(j+k+l+2)}). \tag{32}$$

The evaluation of the approximation is valid only away from the singularities $\sum_{n=0}^{l} \alpha_n x^n = 0$, and along the branch which satisfies the boundary conditions (Shafer, 1974). For the presented rational polynomial representation within a quadrilateral, the α polynomial is a constant and the branch which satisfies the boundary conditions exactly can be determined (see Eq. (29)). Using the irrational polynomial representation a convex polygon with any number of side-nodes and linear boundary conditions can be described. Accordingly higher order behaviors can be modeled on any non-concave two dimensional domain without compromising the smoothness and boundedness requirements necessary for the representation of temperature distributions.

5. Side-node

If the quadrilateral degenerates into an element with a side-node the Wachspress convex polygon method fails. The constant coefficient which weights the side-node becomes zero: $\triangle(2,3,4)=0$. Accordingly, the shape function for the side-node is $N_3(x,y)=0$. Let point $\{x_c,y_c\}$ be the side-node located a distance u along line $\overline{\mathbf{bd}}$:

$$\{x_c,y_c\}=\{x_b,y_b\}(1-u)+\{x_d,y_d\}u. \tag{33}$$

The parametrized coordinate method produces the following coefficients:

$$\begin{aligned}
&\alpha = u(1-u),\\
&\beta(x,y) = u\frac{\triangle(\vec{x},a,b)}{\triangle(d,a,b)}+(1-u)\frac{\triangle(\vec{x},d,a)}{\triangle(b,d,a)}-1,\\
&\gamma(x,y) = \frac{\triangle(\vec{x},d,a)}{\triangle(b,d,a)}\frac{\triangle(\vec{x},a,b)}{\triangle(d,a,b)}.
\end{aligned} \tag{34}$$

Choose the branch which satisfies the nodal point values (see Eq. (29)). Test to make sure this side-node formulation satisfies the shape function conditions, Eqs. (1), (2) and (4).

Evaluating at the nodal points (note $0<u<1$):

$$\begin{aligned}
&\phi_c(x_a,y_a)=\frac{1-\sqrt{1}}{u(1-u)}=0, \quad \phi_c(x_b,y_b)=\frac{u-\sqrt{u^2}}{u(1-u)}=0,\\
&\phi_c(x_c,y_c)=\frac{2u(1-u)-\sqrt{0}}{2u(1-u)}=1, \quad \phi_c(x_d,y_d)=\frac{(1-u)-\sqrt{(1-u)^2}}{2u(1-u)}=0.
\end{aligned} \tag{35}$$

Along the boundary, the coefficient $c(x,y)$ is zero valued along the boundaries from point-(a) to point-(b) and from point-(d) to point-(a):

$$\beta(x,y)-\sqrt{\beta(x,y)^2}=0, \quad \forall\ \beta(x,y)\geqslant 0 \quad \text{and} \quad \alpha\neq 0. \tag{36}$$

Along the boundary from point-(b) to point-(d):

$$\frac{(t+u-2ut)-|t-u|}{2u(1-u)}, \tag{37}$$

the function is zero when $t=0$ and $t=1$, single valued at $t=u$ and otherwise linear along the boundary.

Solving for the remaining shape functions using the same method as for $\phi_c(x,y)$, find:

$$\begin{aligned}
&\phi_a(x,y)=\frac{\triangle(\vec{x},b,d)}{\triangle(a,b,d)}, \quad \phi_b(x,y)=\frac{\triangle(\vec{x},d,a)}{\triangle(a,b,d)}-(1-u)\phi_c(x,y) \quad \text{and}\\
&\phi_d(x,y)=\frac{\triangle(\vec{x},a,b)}{\triangle(a,b,d)}-u\phi_c(x,y).
\end{aligned} \tag{38}$$

The constant and linear fields can be reproduced according to Eq. (4).

The formulation applies even when the side-node and vertex node overlap. If the side-node degenerates into a triangle then the constant $\alpha=0$. The resulting shape function is valid. It satisfies the boundary conditions and is bounded.

$$u=1: \quad \phi_a(x,y)=\frac{\triangle(\vec{x},b,c)\triangle(\vec{x},c,d)}{\triangle(d,b,c)(\triangle(d,b,c)-\triangle(\vec{x},c,d))}. \tag{39}$$

Only the boundary point where $d=c$ is ill behaved.

5.1. Extended side-node formulation

The requirements for a general construction of the side-node formulation are boundedness and the linearity requirement (see Eq. (4)). Eq. (34) can be rewritten such that the shape functions depend only on the parameter u and the shape functions for the triangle $N_i(\vec{x})$. Consequently, the extent to which the conditions are satisfied depends on the shape functions for the 3-noded triangle without a side-node.

$$N_i(\vec{x}) = \frac{\triangle(\vec{x}, j, k)}{\triangle(i, j, k)} \quad \text{where } 0 \leqslant N_i(\vec{x}) \leqslant 1 \text{ for all points } \vec{x} \text{ in the triangle } \triangle(i, j, k). \tag{40}$$

The shape functions $N_i(x, y)$ are single valued only at each named node (i). On all boundary edges which are not adjacent to node (i) the value of the function $N_i(x, y)$ is zero. Any shape function ϕ_i which is similarly bounded and satisfies these boundary conditions on a domain Ω can be used to construct a bounded and smooth shape function for any side-node located on the boundary of Ω.

The four-noded triangle formulation can be extended to any domain where the shape functions for the parent element, without the side-node, is known (see Fig. 7). The shape function for the first side-node is defined in terms of the vertex nodes which share the boundary with the side-nodes.

$$\phi_k = \frac{(1-(1-u)\phi_i^* - u\phi_{i-1}^*) - \sqrt{(1-(1-u)\phi_i^* - u\phi_{i-1}^*)^2 - 4u\phi_{i-1}^*(1-u)\phi_i^*}}{2u(1-u)}. \tag{41}$$

The new shape functions for the parent nodes are updated with respect to the side-node:

$$\phi_i = \phi_i^* - (1-u)\phi_k \quad \text{and} \quad \phi_{i-1} = \phi_{i-1}^* - u\phi_k. \tag{42}$$

No other shape functions are affected. The integration method applied to the encompassing shape without side-nodes can be applied directly to the domain. The discontinuity in slope occurring at the side-node does not prevent integration. Applying this method recursively allows for the representation of any number of side-nodes on any n-gon figure (see Figs. 8–10 and the example in Appendix A.4).

The discriminant is positive if ϕ_i^* and ϕ_{i-1}^* are appropriate shape functions for the parent element:

$$(1-(1-u)\phi_i^* - u\phi_{i-1}^*)^2 \hat{>} 4u\phi_{i-1}^*(1-u)\phi_i^*. \tag{43}$$

If the parent functions are smooth, bounded and linear on the boundary and single valued only at their respective named nodes, then their sum must be bounded:

$$0 \leqslant \phi_i^* + \phi_{i-1}^* \leqslant 1. \tag{44}$$

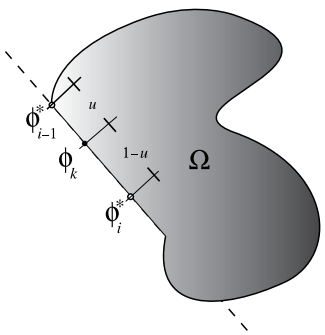

Fig. 7. Side-node shape functions.

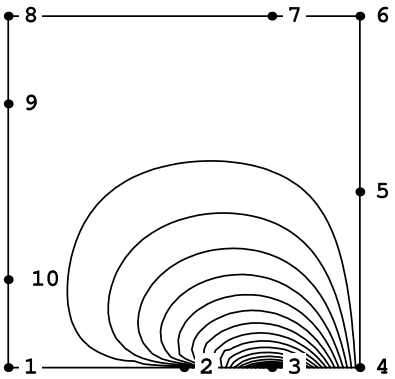

Fig. 8. One side-node influence.

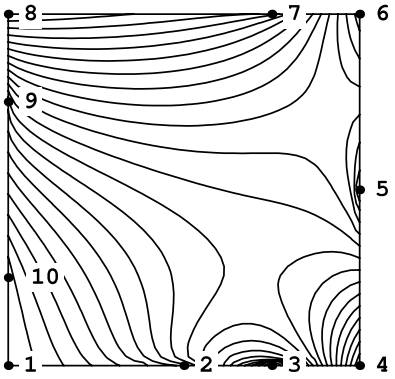

Fig. 9. Many influences.

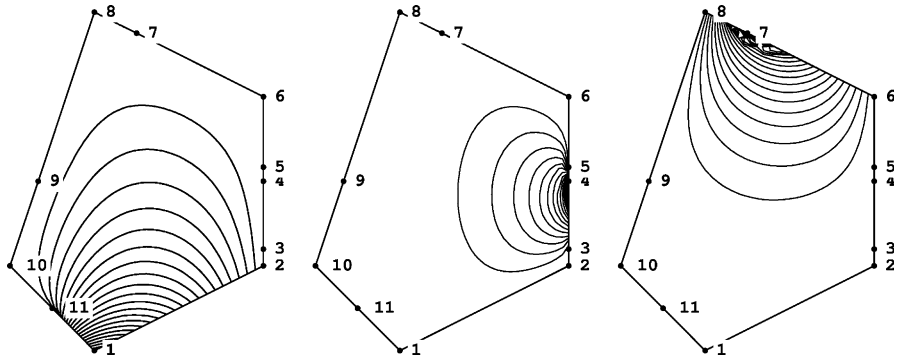

Fig. 10. Selected shape functions for a pentagonal element with side-nodes.

The parameter u is necessarily bounded between 0 and 1 (see Eq. (33)). The worst comparison occurs for the largest values for the shape functions, let $\phi^*_{i-1} = s$ and largest $\phi^*_i = (1-s)$:

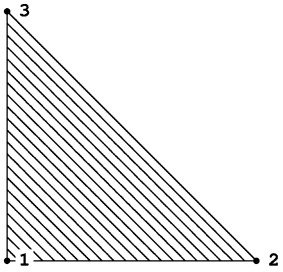

nodes: $\{\{0,0\},\{1,0\},\{0,1\}\}$

$$1-x-y$$

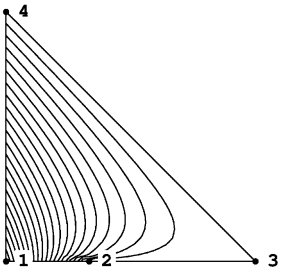

nodes: $\{\{0,0\},\{\frac{1}{3},0\},\{1,0\},\{0,1\}\}$

$$\frac{1-3\,x-4\,y+\sqrt{9\,x^2+6\,x\,(-1+2\,y)+(1+2\,y)^2}}{2}$$

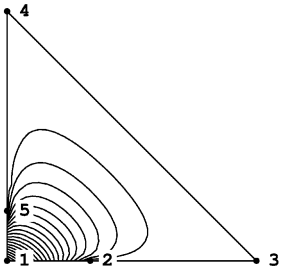

nodes: $\{\{0,0\},\{\frac{1}{3},0\},\{1,0\},\{0,1\},\{0,\frac{1}{5}\}\}$

$$\frac{-7\,(x+y)}{2}+\frac{\sqrt{9\,x^2+6\,x\,(-1+2\,y)+(1+2\,y)^2}}{2}$$

$$+\frac{\sqrt{16\,x^2+(1-5\,y)^2+8\,x\,(1+5\,y)}}{2}$$

Fig. 11. Shape functions for the vertex of a triangle.

$$(1-(1-u)(1-s)-us)^2 \geqslant 4u(1-u)s(1-s). \tag{45}$$

The expression simplifies to:

$$(s-u)^2 \geqslant 0. \tag{46}$$

The discriminant is greater than zero throughout the domain and equal to zero only at the side-node where $s=u$. Consequently any interpolations which are smooth and bounded over a given domain can be combined to construct the shape function for any side-node. For an example construction see Figs. 11 and 12.

6. Conductivity matrix

Convergent shape functions and consistent strain matrices can be formulated for all non-concave quadrilaterals. For the temperature distribution application, the governing operator is the Laplacian.

$$\nabla^2 u(x,y)=0. \tag{47}$$

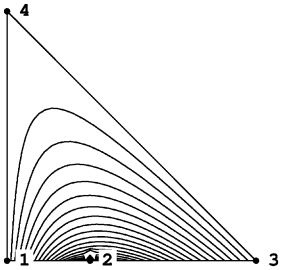

$$\text{nodes: } \{\{0,0\},\{\tfrac{1}{3},0\},\{1,0\},\{0,1\}\}$$

$$\frac{-3\left(-1-x-2\,y+\sqrt{9\,x^2+6\,x\,(-1+2\,y)+(1+2\,y)^2}\right)}{4}$$

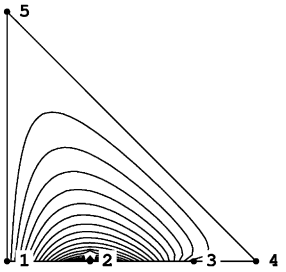

$$\text{nodes: } \{\{0,0\},\{\tfrac{1}{3},0\},\{\tfrac{3}{4},0\},\{1,0\},\{0,1\}\}$$

$$\frac{1+27\,x+34\,y}{20}$$

$$-\frac{17\sqrt{9\,x^2+6\,x\,(-1+2\,y)+(1+2\,y)^2}}{20}$$

$$+\frac{\sqrt{2}}{20}\sqrt{\begin{array}{c}145-360\,x+225\,x^2\\+132\,y+252\,x\,y+196\,y^2\\+(-17+21\,x-98\,y)*\\\sqrt{9\,x^2+6\,x\,(-1+2\,y)+(1+2\,y)^2}\end{array}}$$

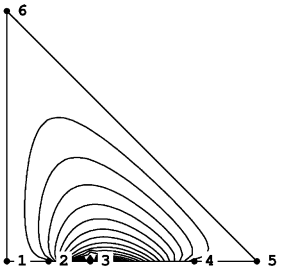

$$\text{nodes: } \{\{0,0\},\{\tfrac{1}{6},0\},\{\tfrac{1}{3},0\},\{\tfrac{3}{4},0\},\{1,0\},\{0,1\}\}$$

$$\frac{-13+39\,x+58\,y}{40}$$

$$-\frac{39}{40}\sqrt{9\,x^2+6\,x\,(-1+2\,y)+(1+2\,y)^2}$$

$$+\frac{\sqrt{2}}{20}\sqrt{\begin{array}{c}145-360\,x+225\,x^2\\+132\,y+252\,x\,y+196\,y^2\\+(-17+21\,x-98\,y)*\\\sqrt{9\,x^2+6\,x\,(-1+2\,y)+(1+2\,y)^2}\end{array}}$$

$$+\frac{\sqrt{2}}{8}\sqrt{\begin{array}{c}5-42\,x+153\,x^2\\+80\,y+276\,x\,y+148\,y^2\\+(3-45\,x-70\,y)*\\\sqrt{9\,x^2+6\,x\,(-1+2\,y)+(1+2\,y)^2}\end{array}}$$

Fig. 12. Shape functions for the side-node of a triangle.

The heat sources applied along the boundary are given by a function $f(t)$ where t is a parameter which travels along the boundary of the polygon. Along a given side ij:

$$x = t^{(ij)}x_i + (1-t^{(ij)})x_j \quad \text{and} \quad y = t^{(ij)}y_i + (1-t_{ij})y_j. \tag{48}$$

Let the heat distribution $u(x,y)$ be approximated by an interpolation function N_i over a polygonal domain with m sides and p side-nodes:

$$u(x,y) \approx \sum_{i=1}^{m+p} u_i N_i(x,y), \tag{49}$$

where, $u_i = u(x_i, y_i)$.

The conductivity matrix is constructed as follows:

$$h_{ij} = \frac{\partial N_i(x,y)}{\partial x}\frac{\partial N_j(x,y)}{\partial x} + \frac{\partial N_i(x,y)}{\partial y}\frac{\partial N_j(x,y)}{\partial y}. \tag{50}$$

Integrating over the domain:

$$S_{ij} = \int_A h_{ij}\,\mathrm{d}A. \tag{51}$$

Integration can be performed over any polygonal domain according to the divergence theorem (Dasgupta, 2003a). Overcoming the algebraic and numerical difficulties associated with integrating a function containing boundary singularities on a convex domain is the subject of further research. Only examples on square domains are presented.

The conductivity matrix constructed from such a formulation is defined by $n-1$ positive eigenvalues and one zero eigenvalue corresponding to the constant temperature condition. For problems of heat flow where boundary temperatures, not heat sources, are given the irrational interpolation allows for a smooth and bounded guess as to the interpolation of heat values over any polygonal domain.

6.1. Test case

Let the temperature distribution in a homogenous medium be governed by:

$$\nabla^2 u(x,y) = 0, \tag{52}$$

and boundary conditions

$$u(H,y) = 0, \quad u(0,y) = 0, \quad u(x,0) = \sin\left(\frac{\pi x}{h}\right) \quad \text{and} \quad u(x,L) = 0. \tag{53}$$

The unique solution to this toy problem on a rectangular domain height $H = 1$ and length $L = 1$ is:

$$u(x,y) = \frac{\sin(\pi x)\sinh(\pi(1-y))}{\sinh(\pi)}. \tag{54}$$

See Fig. 13.

An approximate solution, based on four nodal points, can be constructed using the following shape functions:

$$\{(-1+x)(-1+y),\ x-xy,\ xy,\ y-xy\}. \tag{55}$$

The conductivity matrix is:

$$[\mathbf{S}]^4 = \begin{pmatrix} \frac{4}{3} & -\left(\frac{1}{3}\right) & -\left(\frac{2}{3}\right) & -\left(\frac{1}{3}\right) \\ -\left(\frac{1}{3}\right) & \frac{4}{3} & -\left(\frac{1}{3}\right) & -\left(\frac{2}{3}\right) \\ -\left(\frac{2}{3}\right) & -\left(\frac{1}{3}\right) & \frac{4}{3} & -\left(\frac{1}{3}\right) \\ -\left(\frac{1}{3}\right) & -\left(\frac{2}{3}\right) & -\left(\frac{1}{3}\right) & \frac{4}{3} \end{pmatrix}. \tag{56}$$

The eigenvalues are:

$$\mathrm{eig}([\mathbf{S}]^4) \to \{0, 1.33, 2, 2\}. \tag{57}$$

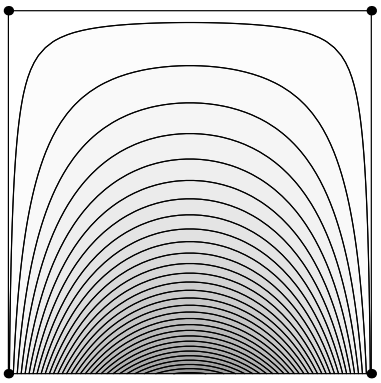

Fig. 13. Exact temperature distribution.

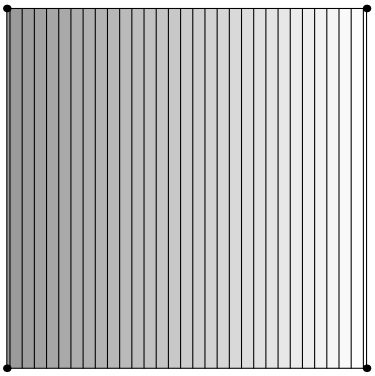

Fig. 14. Four nodes.

The constant temperature case is captured. Matrix [**S**] is singular as expected. The approximation does not capture any quadratic or higher order features of the solution (see Fig. 14).

A five noded element makes a better approximation. The shape functions are:

$$\left\{ \frac{1+2x(-1+y)-3y+\sqrt{-4x(-1+y)^2+4x^2(-1+y)^2+(1+y)^2}}{2}, \right.$$
$$1+y-\sqrt{-4x(-1+y)^2+4x^2(-1+y)^2+(1+y)^2},$$
$$\frac{-1-2x(-1+y)-y+\sqrt{-4x(-1+y)^2+4x^2(-1+y)^2+(1+y)^2}}{2},$$
$$\left. xy,\ y-xy \right\}. \tag{58}$$

The conductivity matrix is:

$$[\mathbf{S}]^5 = \begin{pmatrix} 1.39761 & -0.630998 & -0.247489 & -0.427037 & -0.0920873 \\ -0.630998 & 2.21375 & -0.630998 & -0.475875 & -0.475875 \\ -0.247489 & -0.630998 & 1.39761 & -0.0920873 & -0.427037 \\ -0.427037 & -0.475875 & -0.0920873 & 1.33 & -0.335 \\ -0.0920873 & -0.475875 & -0.427037 & -0.335 & 1.33 \end{pmatrix}. \tag{59}$$

Its eigenvalues are:

$$\mathrm{eig}([\mathbf{S}]^5) \to \{2.79, 2.00, 1.57, 1.32, 0\}. \tag{60}$$

Again the singularity is preserved. The non-linear features of the solution also begin to be represented (see Fig. 15).

The arrangement of nodes need not be symmetric (see Fig. 16). For a six noded element the shape functions are:

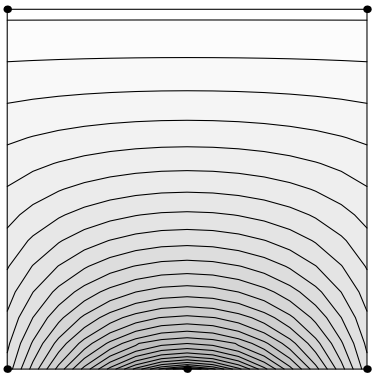

Fig. 15. Five nodes.

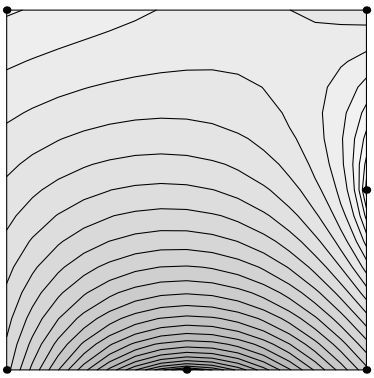

Fig. 16. Six nodes.

$$\left\{ \frac{1+2x(-1+y)-3y+\sqrt{-4x(-1+y)^2+4x^2(-1+y)^2+(1+y)^2}}{2}, \right.$$
$$1+y-\sqrt{-4x(-1+y)^2+4x^2(-1+y)^2+(1+y)^2},$$
$$\frac{-3+x(3-2y)-y+\sqrt{-4x(-1+y)^2+4x^2(-1+y)^2+(1+y)^2}}{2}+\sqrt{1-x+x^2\left(\frac{1}{4}+(-1+y)y\right)},$$
$$\left. 2-x-2\sqrt{1-x+x^2\left(\frac{1}{4}+(-1+y)y\right)},\ -1+x\left(\frac{1}{2}+y\right)+\sqrt{1-x+x^2\left(\frac{1}{4}+(-1+y)y\right)},\ y-xy \right\}. \tag{61}$$

The conductivity matrix is:

$$[\mathbf{S}]^6=\begin{pmatrix} 1.39761 & -0.630998 & -0.124766 & -0.245446 & -0.304315 & -0.0920873 \\ -0.630998 & 2.21375 & -0.377704 & -0.506588 & -0.222581 & -0.475875 \\ -0.124766 & -0.377704 & 1.37868 & -0.719549 & 0.0197986 & -0.176432 \\ -0.245446 & -0.506588 & -0.719549 & 2.95404 & -0.981247 & -0.50121 \\ -0.304315 & -0.222581 & 0.0197986 & -0.981247 & 1.57277 & -0.0843947 \\ -0.0920873 & -0.475875 & -0.176432 & -0.50121 & -0.0843947 & 1.33 \end{pmatrix}. \tag{62}$$

The eigenvalues are:

$$\mathrm{eig}([\mathbf{S}]^6)\rightarrow\{3.73,2.71,1.57,1.5,1.32,0\}. \tag{63}$$

The singularity is preserved.

Any number of side-nodes can be added to improve the solution. For example the eight noded element (Fig. 17) and the 12 noded element, (Fig. 18). The associated eigenvalues of each conductivity matrix is:

$$\mathrm{eig}([\mathbf{S}]^8)\rightarrow\{2.76,2.06,2.06,1.83,1.23,1.08,1.08,0\} \tag{64}$$

and

$$\mathrm{eig}([\mathbf{S}]^{12})\rightarrow\{2.34,2.08,2.08,1.87,1.49,1.28,1.28,1.26,0.99,0.81,0.81,0\}. \tag{65}$$

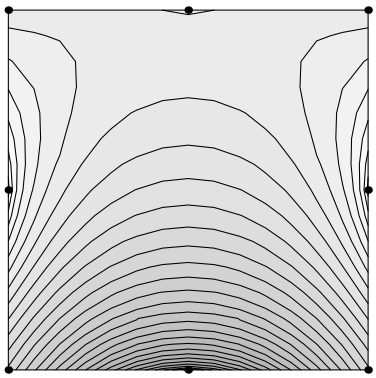

Fig. 17. Eight nodes.

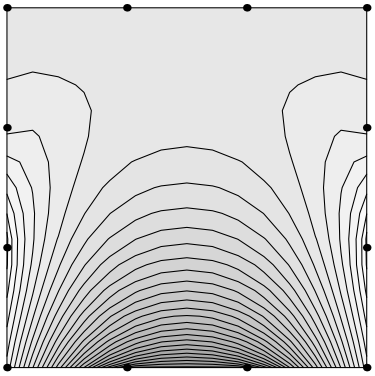

Fig. 18. Twelve nodes.

All of the solutions preserve the zero energy conditions. Notice also the eigenvalues are within the same magnitude and all lie between two positive constants, 1/2 and 4.

A solution constructed using Lagrange interpolates does not preserve the singularity of the conductivity matrix and predicts greater negative values along the boundary:

$$\mathrm{eig}([\mathbf{S}]_I^8) = \{5.33, 4.18, 4.18, 2.57, 1.33, 1.02, 1.02, 0.98\} \tag{66}$$

and

$$\mathrm{eig}([\mathbf{S}]_I^{12}) = \{7.81, 6.46, 6.46, 3.92, 3.38, 2.89, 2.89, 2.53, 1.06, 1.06, 1.03, 1.01\}. \tag{67}$$

The eigenvalues are all positive, but the zero energy condition is not captured. Also the eight node element solution looks qualitatively closer to the actual one than the 12 node element solution does (see Figs. 19 and 20). Also, the positive eigenvalues lie in a wider range, between 1/2 and 8.

All the approximations predict negative values within the domain. For the linear edged approximation, as nodes are added higher order behaviors of the domain are captured and the predicted behavior becomes less negative. The range of values predicted for the temperature distribution over the square domain are presented in Table 2.

For the side-node formulation, as the number of nodes increases the maximum negative value seems to tend to zero and the area over which the solution is negative within the domain decreases. While the

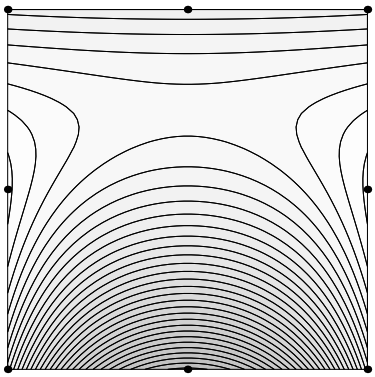

Fig. 19. Eight node.

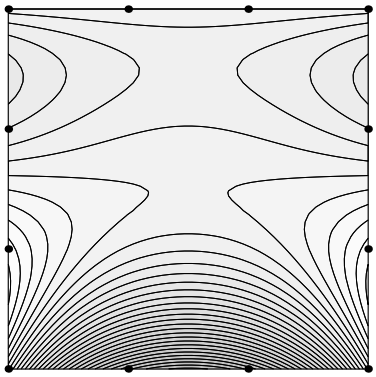

Fig. 20. Twelve node.

Table 2
Range of predicted boundary values

	Side-node formulation	Lagrange element
4 node	$\{-0.32, 0.32\}$	$\{-0.32, 0.32\}$
5 node	$\{-0.23, 0.50\}$	–
6 node	$\{-0.23, 0.54\}$	–
8 node	$\{-0.20, 0.52\}$	$\{-0.25, 1.11\}$
12 node	$\{-0.20, 0.48\}$	$\{-0.22, 0.82\}$

magnitude of the most negative point in the domain for eight node and 12 node representations is equal, much larger segments of the eight node element boundary are negative than the 12 node element. Alternatively, in the Lagrange element formulation the 12 node element contains more negative values in the interior of the domain than the eight node Lagrange element. The Lagrange element converges to the correct solution in an oscillatory manner, this pathology has been observed in other applications as well (MacNeal, 1993).

Also the range of values discovered using the side-node formulation is between 0.64 and 0.88, the range for the Lagrange element is between 0.64 and 1.36 and the maximum value in the solution is 1. In this example the side-node reproduces the bounds of the solution more closely than the Lagrange element method does.

The solutions were constructed using *Mathematica*, the integration is performed algebraically for the four node case and numerically using Gaussian Quadrature for the more than four node cases. The stability of numerical integration decreases around the singular boundary points. Nevertheless, careful integration can return convergent results. The computation time was equivalent for the Lagrange and exact side-node elements for the given number of nodes.

7. Conclusion

The form of the finite element shape function cannot be limited to a polygonal form if the domain being described is neither triangular nor rectangular. Rational polynomials and square roots of polynomials provide a consistent and conformal shape function basis for non-concave shapes. Consequently, this study

extends the class of elements for which closed form shape functions can be constructed. By resisting tessellation of the domain, a higher order representation is possible. Such elements can be applied to boundary value problems including temperature distributions. Unlike Lagrange element formulations, the singularity of the conductivity matrix is preserved.

Acknowledgement

This research was supported by a National Science Foundation Grant number CMS:0202232.

Appendix A. Examples

The isoparametric transformation in x–y coordinates and the smooth side-node representation can be derived algebraically. Some test cases are included.

A.1. Algebraic transformation

Solving for the shape function for a parallelogram in local Cartesian coordinates, let the points a, b, c and d be located at the following points respectively:

$$\{\{-1,0\},\{0,-1\},\{1,0\},\{0,1\}\}.$$

Using Eq. (19):

$$x=(-1)*\frac{(1-\xi)(1-\eta)}{4}+(1)*\frac{(1+\xi)(1+\eta)}{4}=\frac{\eta+\zeta}{2},$$

$$y=(-1)*\frac{(1+\xi)(1-\eta)}{4}+(1)*\frac{(1-\xi)(1+\eta)}{4}=\frac{\eta-\zeta}{2}.$$

Solving for ξ and η in terms of x and y:

$$\xi=x-y,\quad \eta=x+y \quad \text{and} \quad \xi\eta=x^2-y^2.$$

The shape function is a polynomial.

For the shape function of a trapezoid in local Cartesian coordinates, let the points a, b, c and d be located at the following points respectively:

$$\{\{0,0\},\{4,0\},\{3,1\},\{2,1\}\}.$$

Using Eq. (19):

$$x=\frac{9+\eta+5\xi-3\eta\xi}{4} \quad \text{and} \quad y=\frac{1+\eta}{2}.$$

Solving for η and ξ:

$$\xi=\frac{4-2x+y}{-4+3y},\quad \eta=-1+2y \quad \text{and} \quad \xi\eta=\frac{(4-2x+y)(-1+2y)}{-4+3y}.$$

The shape function is a rational polynomial.

For the shape function of a trapezoid in local Cartesian coordinates, let the points a, b, c and d be located at the following points respectively:

$$\{\{0,0\},\{1,0\},\{2,1\},\{0,2\}\}.$$

Using Eq. (19):

$$x = \frac{(3+\eta)(1+\xi)}{4},$$

$$y = \frac{-(1+\eta)(-3+\xi)}{4}.$$

Solving for η and ξ:

$$\xi = 1 + x + y \pm \sqrt{x^2 + 2x(-2+y) + (2+y)^2},$$

$$\eta = \frac{-4 + x + y \mp \sqrt{x^2 + 2x(-2+y) + (2+y)^2}}{2}$$

and

$$\xi\eta = \frac{-8 + x - 7y \mp 5\sqrt{x^2 + 2x(-2+y) + (2+y)^2}}{2}.$$

The shape function contains the square root of a polynomial, there are two roots.

A.2. Skew quadrilateral by isoparametric transformation and Wachspress formulation

Given a set of test points:

$$\{\{x_a, y_a\}, \{x_b, y_b\}, \{x_c, y_c\}, \{x_d, y_d\}\} = \{\{0,0\}, \{1,0\}, \{3/2, 3/2\}, \{0,1\}\}. \tag{A.1}$$

The shape function $\phi_a(x,y)$ found using parametrized coordinates:

$$\left\{5 + x + y - 2\sqrt{x^2 - 2x(-2+y) + (2+y)^2},\ 5 + x + y + 2\sqrt{x^2 - 2x(-2+y) + (2+y)^2}\right\}. \tag{A.2}$$

The shape function $\phi_a(x,y)$ evaluated at the vertices:

$$\phi_a(x_a, y_a) = \{1, 9\}, \quad \phi_a(x_b, y_b) = \{0, 12\}, \quad \phi_a(x_c, y_c) = \{0, 16\} \quad \text{and} \quad \phi_a(x_d, y_d) = \{0, 12\}. \tag{A.3}$$

Only the first root $\frac{\beta(x,y) - \sqrt{\beta(x,y)^2 - 4\alpha\gamma(x,y)}}{2\alpha}$ satisfies the boundary conditions. The continuous shape function, derived from the Wachspress method, for the convex domain, satisfying all the boundary conditions, and the constancy and linearity requirements is:

$$\phi_a(x,y) = \frac{-((3 + x - 3y)(-3 + 3x - y))}{3(3 + x + y)}. \tag{A.4}$$

Consequently, two different valid interpolations can be constructed.

A.3. Triangle with four nodes

$$\{\{-1, 0\}, \{-1/2, 1/4\}, \{1/2, 3/4\}, \{0, 2\}\}. \tag{A.5}$$

The associated shape functions are:

$$\begin{aligned}
\phi_a(x,y) &= \frac{-1-4x-4y+\sqrt{3}\sqrt{-5+4x(1+3x)+16y}}{6},\\
\phi_b(x,y) &= \frac{11+2x+8y-3\sqrt{3}\sqrt{-5+4x(1+3x)+16y}}{12},\\
\phi_c(x,y) &= \frac{7+10x-8y+\sqrt{3}\sqrt{-5+4x(1+3x)+16y}}{12},\\
\phi_d(x,y) &= \frac{-1-x+2y}{3}.
\end{aligned} \tag{A.6}$$

The functions are smooth within the triangular domain.

A.4. Unit square example

The parametrization of the domain is the same as for the shape functions of the element free of side-nodes. For example find the shape functions for side-nodes on a unit square from the shape functions at the vertices for an element with no side-nodes, Eq. (20). For the shape function for a side-node on side 1–2, let u be $u = 0$ at node-1 and $u = 1$ at node-2 and vary linearly along the edge. Substituting into Eq. (41) the equation for the side-node is:

$$\phi_u^m(s,t) = \frac{-1+s(1-u+t(-1+2u))}{2u(u-1)} + \frac{\sqrt{1+s^2(-1+t+u)^2+2s(-1+t+u-2tu)}}{2u(u-1)}. \tag{A.7}$$

The corresponding shape functions then left and right of the side-node respectively, according to Eq. (42), are:

$$\begin{aligned}
\phi_u^l(s,t) &= \frac{-1+s(1-t+u)+\sqrt{1+s^2(-1+t+u)^2+2s(-1+t+u-2tu)}}{2u},\\
\phi_u^r(s,t) &= \frac{1+s(-1-t+u)-\sqrt{1+s^2(-1+t+u)^2+2s(-1+t+u-2tu)}}{2(u-1)}.
\end{aligned} \tag{A.8}$$

For $u = 1/2$:

$$\begin{aligned}
\phi_{\frac{1}{2}}^m(s,t) &= 2-s-2\sqrt{1-s+s^2(t-1/2)^2},\\
\phi_{\frac{1}{2}}^l(s,t) &= s(3/2-t)-1+\sqrt{1-s+s^2(t-1/2)^2},\\
\phi_{\frac{1}{2}}^r(s,t) &= s(1/2+t)-1+\sqrt{1-s+s^2(t-1/2)^2}.
\end{aligned} \tag{A.9}$$

To derive another shape function for another side-node to the left of the original placed by u let another parameter v span the distance between the node to the left of the side-node, node-1, and the side-node itself, node-m. Again, substitute into Eq. (41) to find the shape function. An order of complexity added to the basis functions then is the square root term.

References

Courant, R., 1943. Variational methods for the solution of problems of equilibrium and vibrations. Bulletin of the American Mathematical Society 49, 1–23.

Dasgupta, G., 2003a. Integration within polygonal finite elements. ASCE Journal of Aerospace Engineering 16 (1), 9–18.

Dasgupta, G., 2003b. Interpolants within convex polygons: Wachspress' shape functions. ASCE Journal of Aerospace Engineering 16 (1), 1–8.

Haberman, R., 1998. Elementary Applied Partial Differential Equations, third ed. Prentice Hall, New York.

Irons, B., Ahmad, S., 1980. Techniques of Finite Elements. John Wiley and Sons.

MacNeal, R.H., 1993. Finite Elements: Their Design and Performance. Mechanical Engineering. Marcel Dekker, Inc. TA347.f5M36.

Shafer, R.E., 1974. On quadratic approximation. SIAM Journal on Numerical Analysis 11 (2), 447–460.

Taig, I.C., 1961. Structural analysis by the matrix displacement method. Report S017, English Electric Aviation Report, England.

Wachspress, E.L., 1975. A Rational Finite Element Basis. Academic Press.